



Statically improved fungal laccase-mediated biogenesis of silver nanoparticles with antimicrobial applications

Reem M. Alharbi, Shifaa O. Alshammari, Abeer A. Abd El Aty*

Department of Biology, College of Science, University of Hafr Al Batin, Hafr Al Batin, Saudi Arabia.

ARTICLE INFO

Received on: 04/07/2022
Accepted on: 28/10/2022
Available Online: 04/01/2023

Key words:

Laccase enzyme, *Alternaria arborescens* MK629314, central composite design (CCD), antimicrobial activity, silver nanoparticles.

ABSTRACT

Green synthesis of silver nanoparticles (AgNPs) using microbial enzymes has gained great attention owing to its advantages, such as cost-effectiveness, biocompatibility, eco-friendliness, and simplicity, over conventional physical and chemical methods. In our study, the laccase enzyme of an unconventional source like the endophytic strain *Alternaria arborescens* MK629314 was optimized and applied for AgNP biogenesis. *Alternaria arborescens* laccase enzyme production was first improved using a three-factor, five-level central composite design of 20 trails; the low-cost medium of rice bran increased the laccase production to 6.5-fold. Second, the semipurified laccase enzyme was applied as a reducing and capping agent for the synthesis of AgNPs, and all the characteristics of the formed nanoparticles were studied. The applied techniques were transmission electron microscopy, UV-vis spectroscopy, Fourier transform infrared (FTIR), and dynamic light scattering (DLS). The results of all the analyses emphasized the formation of AgNPs. AgNPs biosynthesized from 25% and 50% semipurified enzyme fractions had size ranges of 6.51 ± 5.12 and 2.51 ± 3.45 nm and showed UV-characteristic peaks at wavelengths of 416 and 404 nm, respectively. DLS analysis presented good peaks with particle size means of 96.20 and 82.30 nm and zeta potentials of -58.3 and -98.5 mv. FTIR analysis showed the appearance of distinctive bands at 3,849.22, 3,440.39, 1,637.27, 1,432.85, 1,159.01, 1,031.73, 597.825, and 520.686 cm^{-1} . The well diffusion method showed a good inhibition zone diameter of antibacterial efficiency against *Escherichia coli* and *Staphylococcus aureus* (15–17 mm) and antifungal activity against filamentous fungi *Aspergillus niger* and *Fusarium solani* (11–13 mm). The achieved results add to the growing relevance of *A. arborescens* as a potential applied endophytic fungus used for diverse biomedical applications.

INTRODUCTION

Metal nanoparticles showed immense popularity due to their characteristic physicochemical properties, as well as containing catalyzing, anticancer, antimicrobial, and magnetic properties (Ovais *et al.*, 2018). Silver nanoparticles (AgNPs) are considered one of the most potential researched metal nanoparticles with high biological activities due to their unique physical properties, especially their large surface area, stability, and small tunable size. In addition, AgNPs have many advantages and are greatly demonstrated in the

fields of biotechnology, pharmaceuticals, and medicine (Ammar *et al.*, 2021; Elyamny *et al.*, 2021).

AgNPs are generally synthesized using photochemical, electrochemical, and γ -irradiation hazardous methods, which depend on the application of toxic chemicals, resulting in environmental problems and biological hazards. In recent times, much effort has been focused, by researchers, on preparing AgNPs using green chemistry approaches (Alshammari and Abd El Aty, 2022; Eltarahony *et al.*, 2021; Raju *et al.*, 2014). Enzyme-mediated formation of nanoparticles is one of the recent techniques used for the safe synthesis of nanoparticles. Enzymes can catalyze the biosynthesis of nanoparticles in their active form and by amino acids released from denatured enzymes, where they act as reducing and stabilizing agents in nanoparticle biosynthesis. Also, the enzyme itself may act as a reducing and capping agent in the formation of nanoparticles (Adelere and Lateef, 2016; Sanket

*Corresponding Author

Abeer A. Abd El Aty, Department of Biology, College of Science, University of Hafr Al Batin, Hafr Al Batin, Saudi Arabia.
E-mail: abeerab@uhb.edu.sa

and Das, 2021). Laccase, ligninase, α -amylase, nitrate reductase, cellulase, and sulfite reductase are examples of relevant microbial enzymes in nanoparticle synthesis (Behera *et al.*, 2022; Kumar *et al.*, 2007; Rai and Panda, 2015; Rangnekar *et al.*, 2007; Sanghi *et al.*, 2011).

Laccase (EC 1.10.3.2) is the enzyme superfamily of multicopper oxidases, which is a widely distributed protein family among eukaryotes and prokaryotes (Devasia and Nair, 2016). Laccases are known for their several biological important roles in medicinal applications, organic synthesis, carbohydrate chemistry, polymer chemistry, food industries, bioremediation, and degradation of different recalcitrant compounds (Abd El Aty and Ammar 2016; Bassanini *et al.*, 2021; Mayolo-Deloisa *et al.*, 2020; Sousa *et al.*, 2021). In addition, fungal laccase may also be a talented biocatalyst for the formation of a metal nanoparticle, and very few researches have been carried out on the laccase-catalyzed synthesis of metal nanoparticles (Chaurasia *et al.*, 2022).

In this direction, white-rot fungi were known as a potential source for biosynthesizing metal nanoparticles due to their high excretion of enzymes, such as peroxidases and laccases (Tortella *et al.*, 2008), and some of these species, *Lentinus edodes*, are applied in the formation of AgNPs depending on laccase enzyme secretion (Lateef and Adeeyo, 2015). Moreover, Sanghi *et al.* (2011) demonstrated that the extracellular laccase production by *Phanerochaete chrysosporium* was responsible for the biosynthesis of gold nanoparticles. Also, the laccase from *Paraconiothyrium variabile* was able to form gold nanoparticles (Faramarzi and Forootanfar, 2011).

Currently, using laccase on a commercial scale is limited due to its low productivity in fungal fermentation. For this reason, optimization of the fermentation medium is preferred for high laccase enzyme productivity. The statistical experimental central composite design (CCD) with the analysis of variance (ANOVA) is one of the useful applications which helps to study the maximum number of factors affecting enzyme production at different levels with a minimum number of experiments (Abd El Aty *et al.*, 2016). The results analyzed by a statistically planned experiment of response surface methodology (RSM) have many advantages over those carried out by the traditional one-variable-at-a-time, with less development time and low overall costs of production (Abd El Aty *et al.*, 2018; Shehata and Abd El Aty, 2014).

The number of reports on the eco-safe synthesis of AgNPs from fungal ascomycete enzymes was very limited. Therefore, the main goal of the present study was to evaluate the biosynthesis of AgNPs using the laccase enzyme of the endophytic strain *Alternaria arborescens* MK629314. Economic optimization of the agriculture residue medium, for high laccase production

with low cost, depends on the statistical design (CCD). Finally, AgNPs were characterized and evaluated for their antibacterial and antifungal activities.

MATERIALS AND METHODS

Microorganism and qualitative assay for laccase production

The endophytic fungus *A. arborescens* used in the present study was isolated from medicinal plants of Wadi Abu Matir, Saint Katherine Protectorate, South Sinai, Egypt, and identified based on both morphological and genetic 18S-rDNA analysis and deposited in GenBank with specific accession number MK629314 (Shaheen and Abd El Aty, 2018). The endophytic fungus was screened for laccase production using the guaiacol oxidation qualitative assay (Abd El Aty *et al.*, 2015; Abd El Aty and Mostafa, 2013).

Analysis of the agricultural waste rice bran (RB)

The agricultural waste RB obtained from the local market was evaluated for the macroelements (nitrogen, phosphorus, potassium, calcium, magnesium, and sodium) and microelements (iron, zinc, copper, and manganese) according to that described by Cottenie *et al.* (1982). The total organic carbon and ash were also evaluated in the Unit of Land Resources Evaluation and Mapping, National Research Centre, Cairo, Egypt.

Low-cost production of laccase enzyme

RB is used as a natural culture medium [medium of RB (RBM)] for laccase production by the endophytic fungus *A. arborescens* MK629314. The fermentation medium contained about 2 g of RB and 50 ml of distilled water in a 250 ml flask, with the addition of copper sulfate at a concentration of 1 mM on day 5 to each culture flask as a laccase inducer. The flasks were incubated for 12, 14, and 17 days at a temperature of 28°C under shaking (150 rpm) conditions.

Three-factor five-level CCD

The 3-factor, 5-level CCD of 20 trails was carried out to optimize the low-cost RBM for maximum laccase production. The correlation between the three variables, RB weight (A), CuSO₄ concentration (inducer) (B), and incubation period (C), and enzyme activity (Y) was studied. All three variables were investigated at the low level (−1), zero level (0), and high level (+1), respectively, with $\alpha = 1.682$, as shown in Table 1. Statistical analysis of the model was performed to evaluate the ANOVA, and the quadratic models were represented as a contour. The statistical Design-Expert® 8 software from Stat Ease, Inc., was used for the purpose of matrix construction and analysis.

Table 1. CCD design for optimization of *A. arborescens* MK629314 laccase enzyme production.

Variable code	Variable	Levels				
		− α	−1	0	+1	+ α
A	RB (g/flask)	2.32	3	4	5	5.68
B	CuSO ₄ (mM)	1.32	2	3	4	4.68
C	Incubation period (days)	8.64	10	12	14	15.36

$\alpha = 1.682$.

Laccase assay

According to Mostafa and Abd El Aty (2018), extracellular laccase activity was measured based on the oxidation of the substrate 2,2'-azino-bis(3-ethylbenzothiazoline)6-sulphonic acid (ABTS). One unit of laccase activity was defined as the activity of an enzyme that catalyzes the conversion of 1 μmol of ABTS per minute.

Protein assay

In accordance with Lowry *et al.*'s (1951) description, protein concentration was determined.

Partial purification of laccase enzyme

Fractional precipitation of the laccase enzyme with acetone was applied at three different concentrations of 25%, 50%, and 75%. The specific activity (SA) and purification fold of each fraction were calculated according to the following equations (Abd El Aty *et al.*, 2017):

$$\text{SA} = \text{Enzyme activity "U"/protein content "mg"} \quad (1)$$

$$\text{Purification fold} = \text{SA of partial purified fraction/SA of crude culture filtrate} \quad (2)$$

Applications of laccase enzyme in biosynthesis of nanosilver

The partially purified fractions of laccase (25%, 50%, and 75%) in comparison with the crude enzyme were used for the synthesis of AgNPs. The reaction mixture contains 3 ml of the equal volume of the enzyme fraction and 1 mM AgNO_3 , incubated in a 150 rpm rotating shaker at 30°C–33°C for 24 hours duration in dark conditions.

Characterization studies of biosynthesized AgNPs

The formation of AgNPs was preliminarily indicated by changing the color of the mixture to reddish-brown (Abd El Aty and Ammar, 2016).

UV-visible spectroscopy

The bioreduction of silver ions was monitored by a UV-visible spectrophotometer. The absorption spectrum of the reaction mixture was scanned in the range of 200–700 nm, and the sharp peak given by the UV-visible spectrum at the absorption range of 400–450 nm indicated the formation of AgNPs.

Transmission electron microscopy (TEM)

AgNPs were characterized by TEM (JEOL-2100) to detect the size and shape of nanoparticles. 2 μl of the AgNPs sample was loaded on a formvar-coated 200-mesh copper grid (Ted Pella, Redding, CA), air-dried before examination, and loaded onto a specimen holder. The size and shape of AgNPs were clarified from the TEM micrographs.

Dynamic light scattering (DLS)

A DLS was used for the analysis of the hydrodynamic diameter of particles and distribution of particles in solution. The distribution of solid particles of nanosilver in the liquid solution was determined by Nicomp Particle Sizing Systems CW388 (Nicomp 380, Inc., Santa Barbara, CA). Zetasizer Nano ZS

ZEN3600 (Malvern Instruments Ltd., Worcestershire, UK) was used to analyze the AgNPs' hydrodynamic diameters.

Fourier transform infrared (FTIR) spectroscopy

FTIR (JASCO, FT/IR-6100) was used to detect the structural characteristic and functional groups of the nanosilver solution. The peaks were recorded by drop-coating AgNPs solution into a KBr disk under a hydraulic press at 10,000 psi. Each KBr disk was scanned at the range of 400–4,000 cm^{-1} and a resolution of 4 cm^{-1} .

Antimicrobial characters of biosynthesized AgNPs

Nanosilver biosynthesized from 25%, 50%, and 75% semipurified enzyme fractions and the crude enzyme was screened *in vitro* against different pathogenic strains of Gram-positive bacteria (*Staphylococcus aureus* ATCC29213), Gram-negative bacteria (*Escherichia coli* ATCC25922), and fungi (*Aspergillus niger* NRC53, *Fusarium solani* NRC15) by the agar well diffusion technique (Ammar *et al.*, 2021; Abd El Aty *et al.*, 2020). Spore suspensions of fungal strains were prepared and adjusted to be approximately 1×10^6 ml, and bacterial cell suspensions adjusted to be approximately 1×10^8 ml. One ml of each suspension was inoculated separately into a plate containing 25 ml of sterile potato dextrose agar and nutrient agar medium, respectively. About 200 μl of AgNPs was added to wells of 10 mm in diameter, and then the plates were left for 30 minutes at room temperature for compound diffusion. The plates were incubated for 24 hours at 30°C for bacteria and 72 hours at 28°C for fungi. The inhibition zones of all tested organisms were recorded in millimeters (mm) at three different points, and the average values were reported as mean \pm SD using MS Excel.

RESULTS AND DISCUSSION

Laccase enzyme production

Alternaria arborescens MK629314 has a good ability to oxidize guaiacol; as shown in Figure 1A, a reddish-brown zone formed under and around a 10 mm fungal disk indicating the production of the laccase enzyme. The endophytic fungus *A. arborescens* MK629314 showed the ability to produce an appreciable amount of the laccase enzyme (41.05 U/ml) after incubation for 12 days in an RB medium under shaking conditions of 150 rpm (Fig. 1B). The analysis study of RB agricultural waste indicated that it contains many valuable nutrients of (9.44%) protein, (86%) organic carbon, (2.3%) phosphorus, (1.51%) nitrogen, (0.8%) potassium, (0.65%) magnesium, (240 ppm) calcium, (11,000 ppm) sodium, (380 ppm) iron, (0.384 ppm) manganese, (52 ppm) zinc, (9 ppm) copper, and (14%) ash. The results obtained are in agreement with Chawachart *et al.*'s (2004) study, who found that cultivation of the thermotolerant *Coriolus versicolor* strain RC3 on RB exhibited the highest laccase production compared to glucose, wheat bran, and rice straw. Using RB as an efficient substrate for laccase production may be related to its content of phenolic compounds (ferulic acid and vanillic acid), which were reported as inducers for laccase production (Munoz *et al.*, 1997). On the other hand, the lignocellulosic substrate wheat straw was found

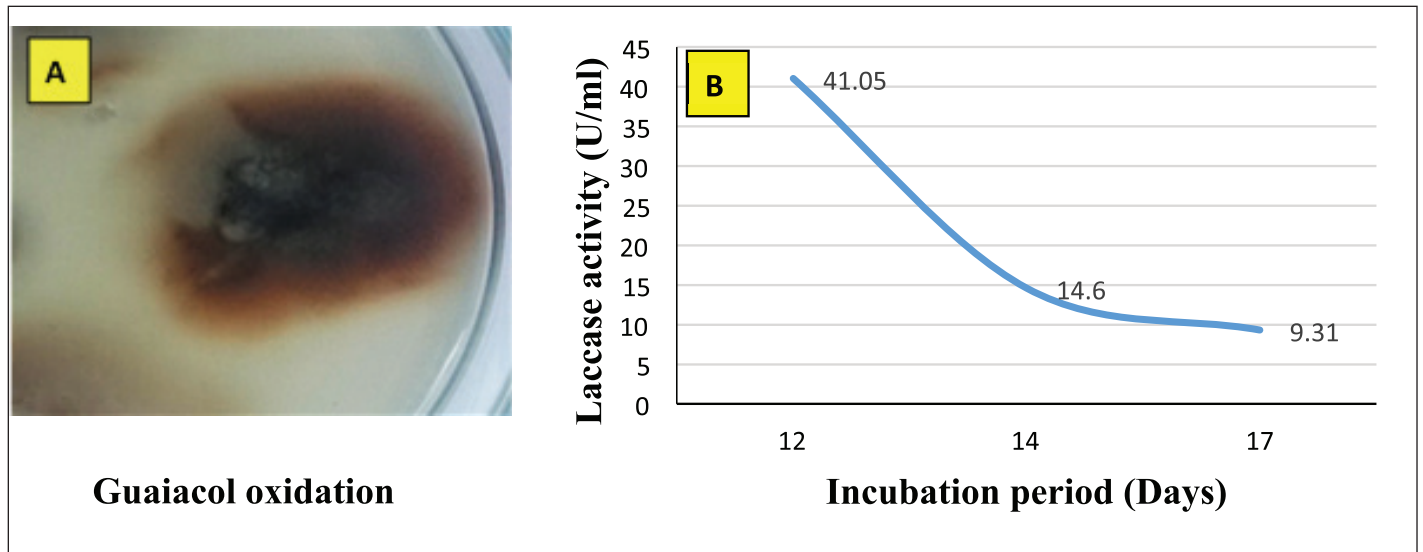


Figure 1. (A) Qualitative assay of *A. arborescens* MK629314 laccase production and (B) quantitative production of laccase enzyme using RB medium at different incubation periods.

to be the most suitable for laccase production using *Tricholoma giganteum* AGHP (Patel and Gupte, 2016).

Optimization of *A. arborescens* MK629314 laccase production

The economic production medium (RBM) of the laccase enzyme was optimized using the RSM of CCD. The combined effect of factors tested RB weight (A), CuSO_4 concentration (B), and incubation period (C), and was optimized using a three-factor, five-level CCD with 20 trails for maximum laccase production. In Table 2, all the observed and predicted values of responses along with the matrix of the design were shown; the lowest response of 59.14 U/ml enzyme activity was obtained at long period incubation for 15 days with 4 g/flask RB and 3 mM CuSO_4 concentration. On the other hand, the highest response of 266.65 U/ml enzyme activity was noticed in the experimental trial of 4 g/flask RB, 3 mM CuSO_4 , and an incubation period of 9 days. Various response values of laccase activity obtained with different factors' concentrations and different interactions validate the applied CCD in accordance with a previous study (Eltarhony *et al.*, 2020).

The results obtained indicated the great effect of incubation time, where the proteins may lose a significant amount of their catalytic activity over the long period of incubation, as indicated by Muthukumarasamy *et al.* (2015), who obtained the maximum laccase enzyme from *Bacillus subtilis* MTCC 2414 by using RB (267 ± 2.64 U/ml) as a substrate with a 96 hours incubation period, but the enzyme activity declined at a higher incubation time of 144 hours.

In comparison with the basal medium, the statistical design indicated that increasing the RB weight and CuSO_4 concentration to 4 g/flask and 3 mM, respectively, with a 9-day incubation period is more favorable for high laccase production. After the application of RSM, it was obvious that a 6.5-fold improvement in laccase enzyme production was being achieved. This result emphasized the value and necessity of applying the statistical optimization design.

The following quadratic model Equation (3) in terms of coded factors was given by the multiple regression analysis of the experimental data:

$$Y \text{ activity (U/ml)} = +188.07 + 12.38 * A - 20.94 * B - 43.32 * C + 4.97 * A * B + 1.59 * A * C + 15.42 * B * C - 37.35 * A^2 - 2.11 * B^2 - 6.98 * C^2 \quad (3)$$

Y activity was the response (laccase activity). A–C were the code values of the tested variables (RB, CuSO_4 , and incubation period, respectively). The regression equation was graphically represented by the three-dimensional response surface and the two-dimensional contour plots for understanding the interaction effects of the independent factors on the response value (Figs. 2 and 3).

Figures 2 and 3A–C show the response surface of RB and CuSO_4 at C = 0 (A), RB and incubation period at B = 0 (B), and CuSO_4 and incubation period at A = 0 (C) on laccase activity, respectively, keeping the other components at the fixed zero level. The 3D plot showed that when the concentrations of RB and CuSO_4 increased, the enzyme activity gradually increased until it reached the center point, and the elliptical 2D contour plot confirmed the significant synergistic interaction between the two factors (Fig. 3A).

Ibrahim *et al.* (2022) demonstrated that the contour plot shape usually points out the nature and extent of the interactions between the tested variables. In this context, a circular contour plot (Fig. 3B and C) reveals an insignificant interaction between the incubation period and concentrations of RB and CuSO_4 . Maximum laccase activity could be achieved by increasing the concentration of RB and CuSO_4 while decreasing the incubation period.

The satisfactory correlation between the actual (experimental) and predicted values of laccase enzyme activity (R) showed as clusters near the diagonal line. The parity plot indicated a suitable fit of the model (Fig. 4).

Table 2. RSM of CCD of predicted and experimental values of enzyme production.

Trials	RB (A, g/flask)	CuSO ₄ (B, mM)	Incubation period (C, days)	Laccase activity U/ml)	
	Levels	Levels	Levels	Experimental	Predicted
1	- α	0	0	81.57 \pm 1.62	61.62
2	+ α	0	0	72.40 \pm 1.87	103.26
3	-1	-1	+1	95.09 \pm 12.18	94.83
4	+1	-1	+1	144.79 \pm 3.61	112.84
5	-1	+1	-1	108.60 \pm 9.07	132.84
6	0	0	0	188.39 \pm 8.34	188.07
7	0	0	0	188.39 \pm 8.34	188.07
8	0	- α	0	213.62 \pm 7.03	217.32
9	0	0	0	188.39 \pm 8.34	188.07
10	0	0	0	188.39 \pm 8.34	188.07
11	0	0	+ α	59.14 \pm 2.74	95.48
12	+1	+1	-1	171.81 \pm 7.08	164.37
13	-1	+1	+1	85.91 \pm 3.18	73.85
14	0	+ α	0	139.70 \pm 2.61	146.89
15	+1	-1	-1	222.79 \pm 6.59	227.15
16	+1	+1	+1	134.85 \pm 5.11	111.75
17	-1	-1	-1	200.11 \pm 5.97	215.51
18	0	0	0	188.39 \pm 8.34	188.07
19	0	0	- α	266.65 \pm 5.09	241.21
20	0	0	0	188.39 \pm 8.34	188.07

ANOVA indicated that the applied model is highly significant, as represented in Table 3. The analysis indicated that the model's *F*-value of 10.42 implies the model is significant. There is only a 0.05% chance that a "model *F*-value" this large could occur due to noise. In addition, goodness of fit and suitability of the model were also shown from the high values of $R^2 = 0.9037$ and Adj $R^2 = 0.8170$.

Values of "Prob > *F*" less than 0.0500 indicate that model terms are significant. In this case, B, C, and A2 are significant model terms. In Figure 3, the relationship between the expected and actual values of laccase activity was shown. The cluster of calculations formed near the diagonal line in the plot showed the goodness of fit of the model and indicated an excellent correlation between the expected and actual values.

The validation was carried out with the optimum fermentation conditions, RB 4 g/flask with the addition of 3 mM CuSO₄, and incubated for 9 days. The actual value of laccase production (266.65 U/ml) was observed, which is to some extent closer to the predicted value (241.21 U/ml). The obtained results emphasized the effectiveness and validity of the applied experimental model.

Precipitation of the laccase enzyme by acetone

Alternaria arborescens laccase was partially purified from the culture filtrate by acetone at 25%, 50%, and 75% concentrations. Figure 5 shows a good purification fold (3.14) with 50% acetone, followed by a purification fold (1.36) at 25% acetone and 75% acetone, which showed the highest recovered protein and the lowest purification fold (0.49).

Biosynthesis of nanosilver using laccase enzyme

The semipurified enzyme fractions precipitated at 25%, 50%, and 75% acetone and crude enzyme were applied for AgNP biosynthesis. The formation of nanosilver was firstly detected by optical characterization, where the color of the solution mixture was changed from a pale yellow to reddish color with different degrees (Fig. 6). The change in color formed as the result of the silver ions reduction by the laccase enzyme. Also, the variation between the four mixtures is due to the difference between the biomolecules involved in the biosynthesis of AgNPs, in addition to the surface plasmon excitation in nanoparticles (Chaurasia *et al.*, 2022; Mulvaney, 1996; Lateef and Adeeyo, 2015).

Characterization of AgNPs

The biosynthesized AgNPs were further characterized by a UV-visible spectrophotometer. AgNPs were scanned in ranges from 200 to 700 nm. The result obtained indicated the surface plasmon resonance of AgNPs biosynthesized by 25%, 50%, and 75% appearing at wavelengths of 416, 404, and 400 nm, respectively, which is considered a characteristic plasmon peak for AgNPs (Shaheen and Abd El Aty, 2018). No characterized peak formed by using the crude enzyme at the absorption range of 400–450 nm, indicating the absence of differentiated nanoparticles, which may be formed according to the color change of the reaction mixture but are unstable and highly aggregated (Fig. 7). This observation has further been confirmed by the TEM analysis.

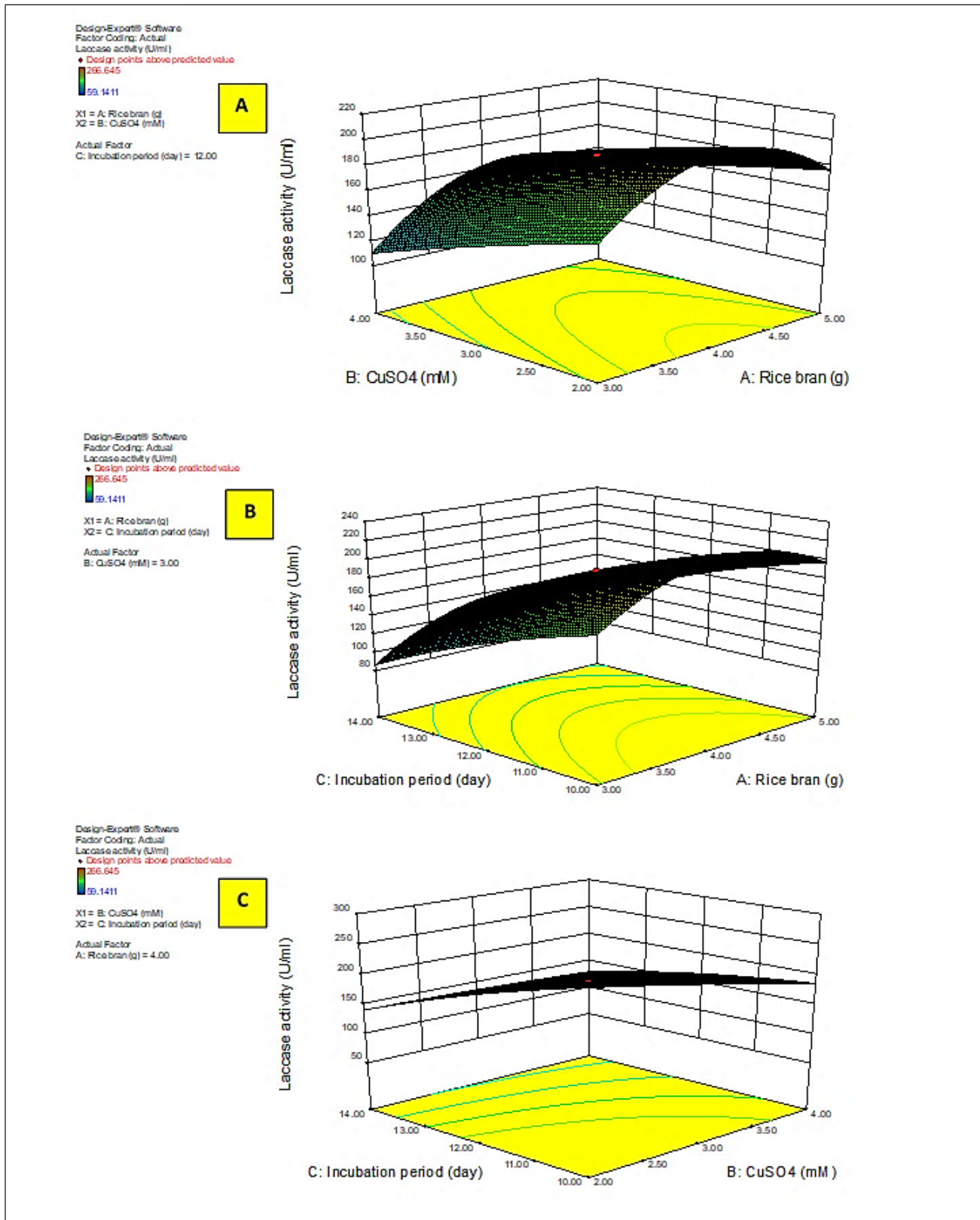


Figure 2. 3D response surface plots of laccase activity by *A. arborescens* showing the interactive effects between independent significant variables.

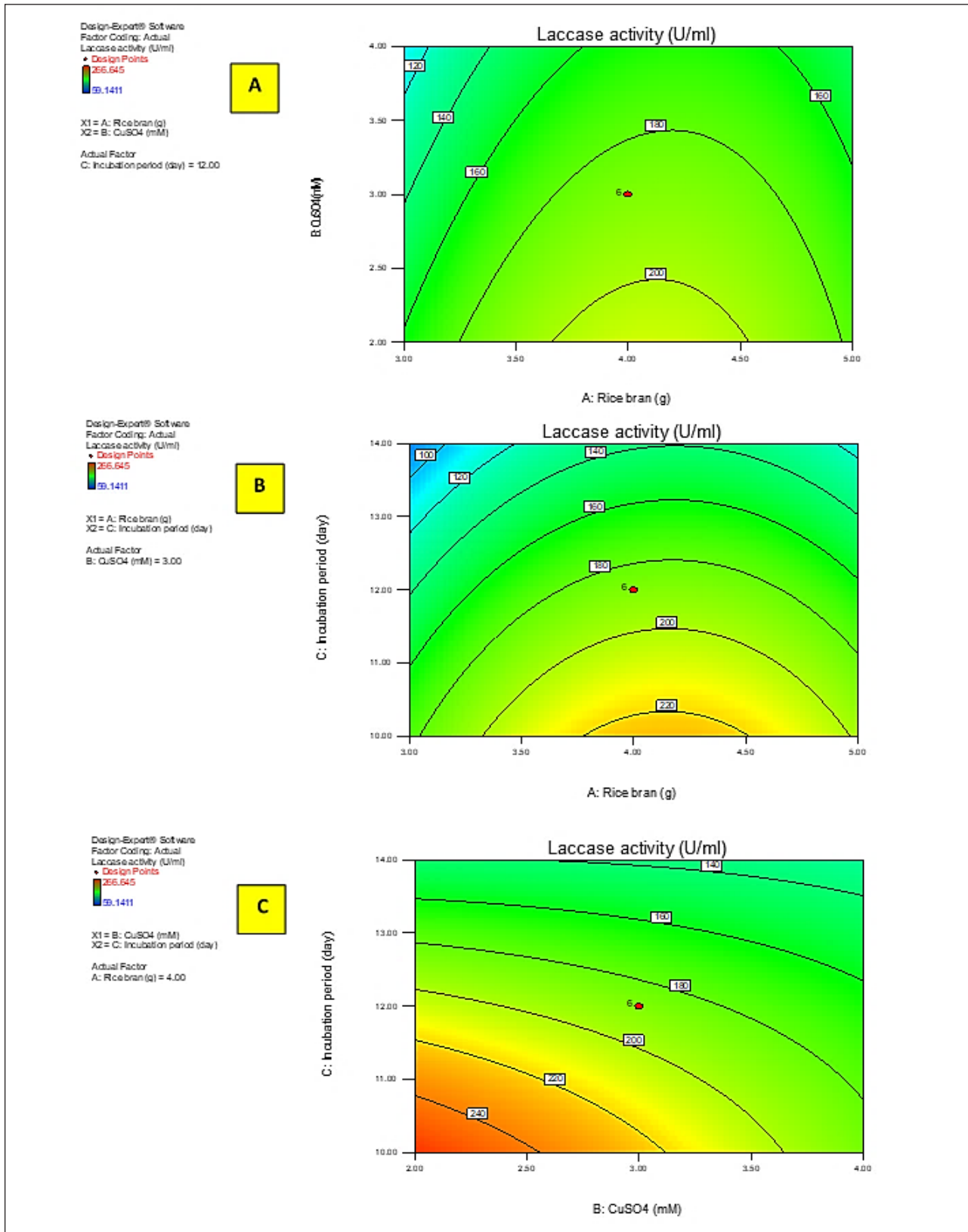


Figure 3. 2D contour plots of laccase activity by *A. arborescens* showing the interactive effects between independent significant variables.

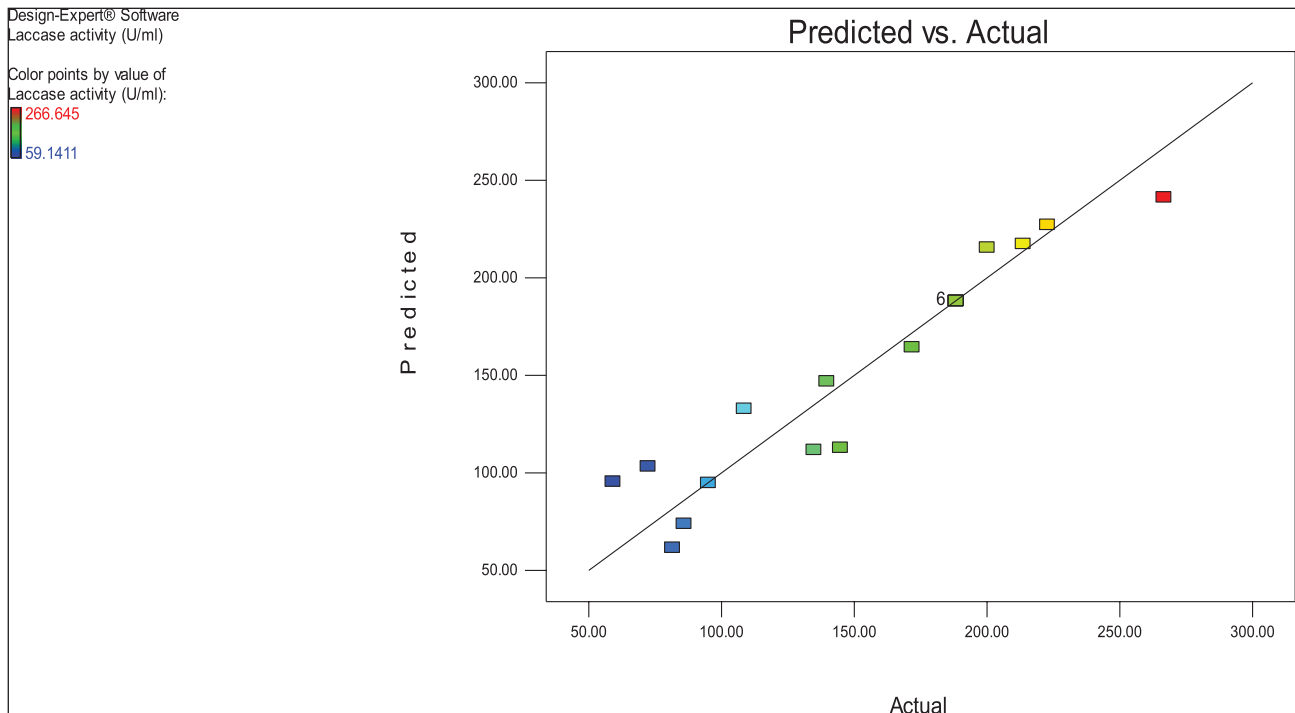


Figure 4. Predicted versus actual laccase activity (U/ml) of the endophytic fungus *A. arborescens*.

Table 3. ANOVA for three-factor, five-level CCD.

Source	Sum of squares	df	Mean square	F-value	p value Prob > F
Model	56,145.61	9	6,238.40	10.42	0.0005 significant
A—RB	2,094.48	1	2,094.48	3.50	0.0909
B—CuSO ₄	5,987.17	1	5,987.17	10.00	0.0101
C—incubation period	25,632.76	1	25,632.76	42.83	<0.0001
AB	197.68	1	197.68	0.33	0.5782
AC	20.31	1	20.31	0.034	0.8575
BC	1,902.85	1	1,902.85	3.18	0.1049
A ²	20,102.34	1	20,102.34	33.59	0.0002
B ²	64.08	1	64.08	0.11	0.7503
C ²	701.21	1	701.21	1.17	0.3045
Residual	5,984.80	10	598.48		
Lack of fit	5,984.80	5	1,196.96		
Pure error	0.000	5	0.000		
Cor. total	62,130.41	19			

SD = 24.46, $R^2 = 0.9037$, mean = 156.37, Adj $R^2 = 0.8170$, CV = 15.65%, Pred $R^2 = 0.2631$, PRESS = 45,786.13, Adeq. precision = 10.382.

The size and structure of AgNPs were analyzed by high rate-TEM. The results showed well-dispersed cubic to rounded particles with different sizes biosynthesized from 25% and 50% semipurified enzyme fractions in the ranges of 6.51 ± 5.12 and 2.51 ± 3.45 nm, respectively (Fig. 8A and B). Various sizes of spherical-shaped AgNPs have been reported in previous studies (Ammar *et al.*, 2021; Abd El Aty and Zohair, 2020). The TEM image of the AgNPs 75% enzyme fraction at 100–200 nm showed some aggregations of AgNPs with a variable size range of 28.65 ± 7.48 nm (Fig. 8C). On the other hand, TEM analysis indicated

the presence of different fungal metabolites in the crude extract interferes with the good reduction and stabilization of the AgNO₃, where the image showed no dispersed nanoparticles (Fig. 8D). The obtained results indicated the importance of the purification process for perfect AgNO₃ reduction and biosynthesis of well-dispersed stable AgNPs.

The best nanoparticles formed with the 25% and 50% semipurified enzyme fractions were more characterized, and a perfect reduction process was confirmed by DLS analysis of the Zetasizer analysis and FTIR spectrum.

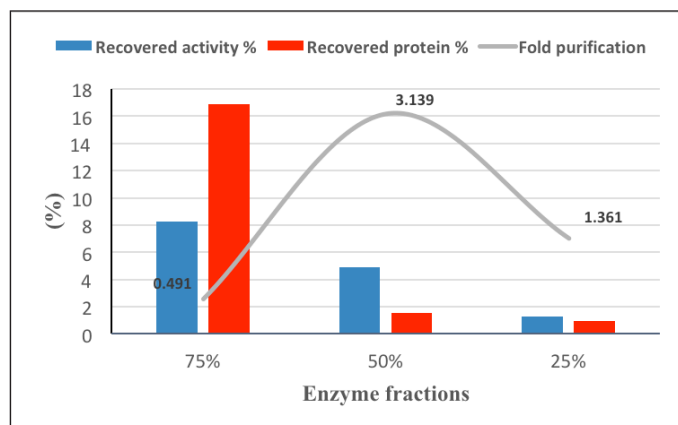


Figure 5. Partial purification of *A. arborescens* laccase by acetone.

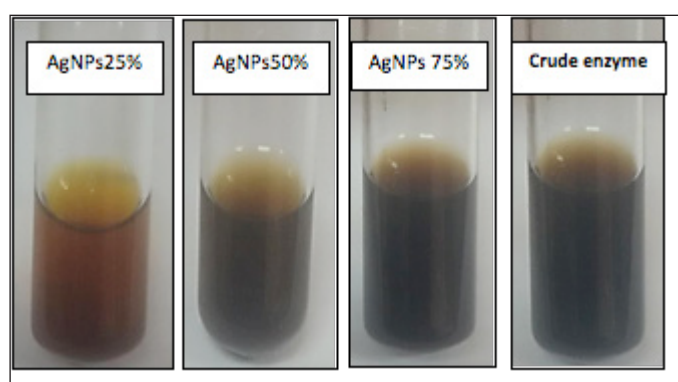


Figure 6. Color change in the solution mixture of AgNPs biosynthesized after mixing the enzyme fraction (25%, 50%, and 75%) and crude enzyme with 1 mM AgNO_3 and incubated at 30°C–33°C for 24 hours under shaking conditions at 150 rpm in dark conditions.

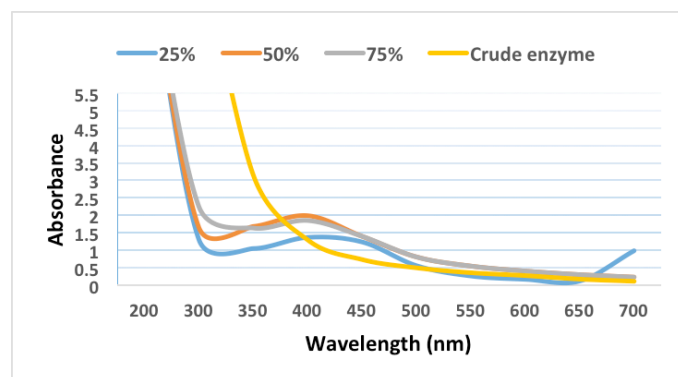


Figure 7. UV-vis spectra analysis of AgNPs synthesized by partially purified laccase enzyme fraction and crude extract.

In this study, the DLS analysis of AgNPs of 25% and 50% presented characteristic peaks with the particle size means of 96.20–82.30 nm, with zeta potentials of -58.3 and -98.5 mv, respectively (Fig. 9). High negative values of dispersed biosynthesized AgNPs of 25% and 50% enzyme fractions appeared clearly to be advantageous for long-term colloidal

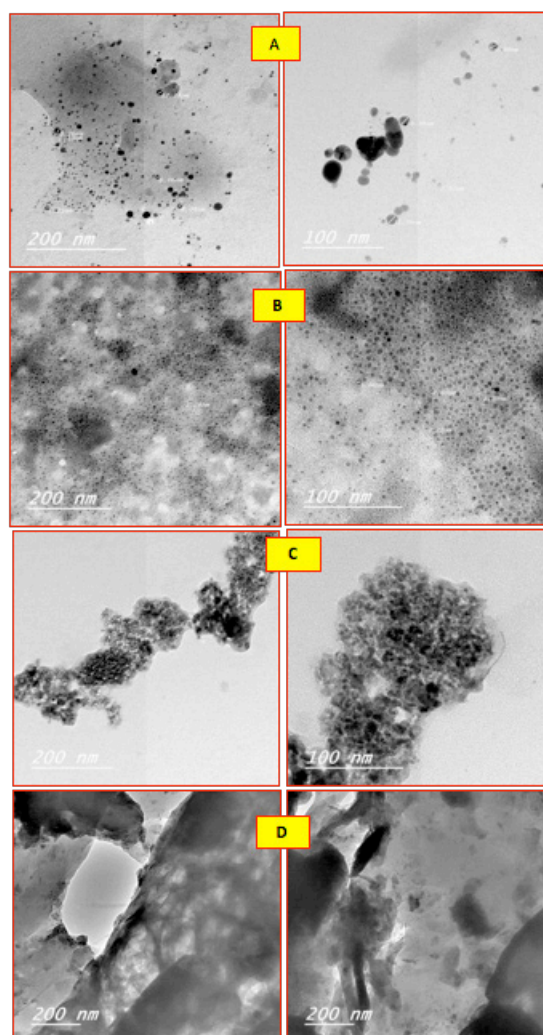


Figure 8. TEM analysis of AgNPs formed by 25% (A), 50% (B), and 75% (C) partially purified laccase enzyme and crude extract (D) showing their shapes, sizes, and distribution, at the magnification views of 100–200 nm.

stability, as mentioned by [Eltarahony *et al.* \(2018\)](#), who indicated that values greater than +25 mV or less than -25 mV display higher electrical charge on nanoparticles surface, which prevents agglomeration and flocculation by the action of potent repulsive forces between the ultrafine particles. On the other hand, [Elyamny *et al.* \(2021\)](#) showed slightly low surface charges (-5.34 mV) of Ag @ Ag_2O NCs, which tend to form aggregations.

In addition, the nanoparticle biosynthesis by 25% and 50% enzyme fractions was extended to analyze their FTIR spectrum. FTIR analysis showed the appearance of distinctive bands at 3,849.22, 3,440.39, 1,637.27, 1,432.85, 1,159.01, 1,031.73, 597.825, and 520.686 cm^{-1} (Fig. 9). The primary amine (NH_2) was indicated by peaks that appeared at 3849.22 and 3,440.39 cm^{-1} ([Shaligram *et al.*, 2009](#)), where the 1,159.01 and 1,031.73 cm^{-1} bands are due to OH and aliphatic amine deformation ([Gopinath and Velusamy, 2013](#)). In addition, the bands that appeared at 1,637.27–1,432.85 cm^{-1} were an indication of hydroxyl group deformation, which in turn causes the silver-

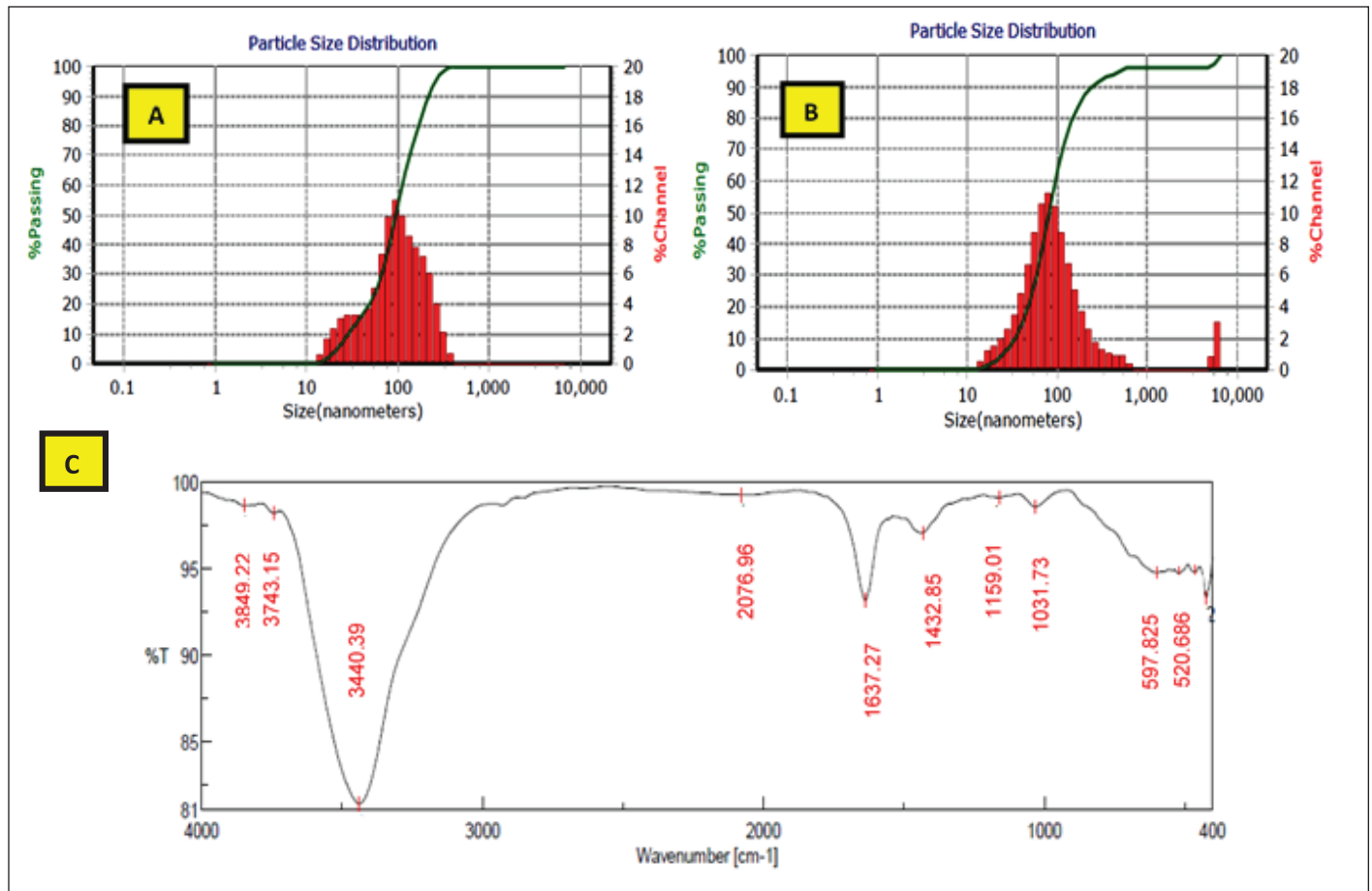


Figure 9. DLS analysis showing particle size distribution of AgNPs biosynthesized by 25% (A) and 50% (B) partially purified enzymes. FTIR spectrum of AgNPs formed by 25% and 50% enzyme fractions (C).

metal ion bioreduction to form nanoparticles (Gopinath and Velusamy, 2013; Thirumurugan *et al.*, 2011). Eltarahony *et al.* (2021) reported that the peaks in the low range of 400–700 cm⁻¹ denote the presence of metals in the examined sample. In the present study, characteristic peaks were observed at 597.825 and 520.686 cm⁻¹ that showed the P–O–C groups in phospholipids and/or S–S stretch band of protein (Eid *et al.*, 2020).

Generally, the following study reflected that the biomolecules of the *A. arborescens* semipurified enzyme were responsible for perfect capping and stabilization of AgNPs, depending on free amine groups in the laccase enzyme proteins, which are able to bind to nanoparticles to protect them from aggregation.

Antibacterial and antifungal activity of AgNPs

AgNPs biosynthesized from different semipurified enzyme fractions were tested against pathogenic bacteria and fungi using the agar well diffusion technique (Fig. 10). The results showed that both AgNPs of 25% and 50% enzyme fractions had good antimicrobial efficiency against all tested pathogens (Table 4). AgNPs 25% and 50% induced a maximum inhibitory zone of 15–17 mm inhibition zone diameter (IZD) against Gram-positive and Gram-negative pathogenic bacteria strains and exhibited the inhibitory activity of 11–13 mm

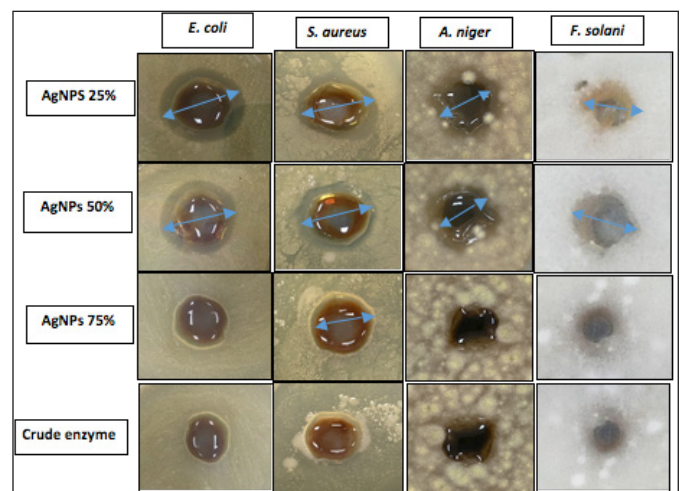


Figure 10. Antimicrobial activity of AgNPs of 25%, 50%, and 75% and crude enzyme against pathogens.

IZD as an antifungal effect against filamentous fungi. It has been reported that AgNPs biosynthesized from extracellular laccase of *L. edodes* showed selective antimicrobial activities against 10 clinical bacterial isolates (Lateef and Adeeyo, 2015). In this

Table 4. Antimicrobial assay of biosynthesized AgNPs against pathogens.

Treatment	IZD (mm)			
	Gram –ve bacteria	Gram +ve bacteria	Fungi	
	<i>E. coli</i> ATCC25922	<i>S. aureus</i> ATCC29213	<i>A. niger</i> NRC53	<i>F. solani</i> NRC15
AgNPs 25%	17 ± 0.92	15 ± 0.71	11 ± 0.14	13 ± 0.92
AgNPs 50%	16 ± 0.06	15 ± 0.14	11 ± 0.78	13 ± 1.21
AgNPs 75%	ND	12 ± 0.83	ND	ND
Crude enzyme	ND	ND	ND	ND

context, AgNPs synthesized from xylanases of *A. niger* L3 (NEA) and *Trichoderma longibrachiatum* L2 (TEA) inhibited the growth of bacteria (*E. coli*, *Klebsiella granulomatis*, *S. aureus*, and *Pseudomonas aeruginosa*) and fungi (*A. niger*, *Aspergillus flavus*, and *Aspergillus fumigatus*) (Elegbede *et al.*, 2018).

The obtained results showed that all tested pathogens, *E. coli*, *A. niger*, and *F. solani*, are able to resist AgNPs of 75% and the crude enzyme, except *S. aureus*, which showed a weak IZD of 12 mm. Bhat *et al.* (2011) emphasized the bactericidal effect of AgNPs depending on the nanoparticle size. The obtained results are in agreement with this study's findings, where small-sized AgNPs of 25% and 50% in the ranges of 6.51 ± 5.12 and 2.51 ± 3.45 nm, respectively, with a larger surface area can easily interact with containing constituents (sulfur and phosphorus) of the bacterial cell causing cell killing by attacking the respiratory chain and cell division in accordance with Lateef *et al.* (2016).

AgNPs of 25% and 50% showed zeta potential of high negative charges (–58.3 and –98.5 mV) on their surface, directly resulting in an interaction of these charges with the electric charge present on the surfaces of the microbes. Generally, this effect seems to be the most important factor affecting AgNPs antimicrobial activities (Ammar *et al.*, 2021).

CONCLUSION

This work showed the first report on *A. arborescens* laccase enzyme-mediated synthesis of AgNPs. The laccase enzyme of *A. arborescens* endophytic fungus was economically improved and optimized through a three-factor, five-level CCD of an economic agricultural waste medium. Application of RSM improved enzyme production to 266.65 U/ml in the experimental trial of 4 g/flask RB, 3 mM CuSO₄, and an incubation period of 9 days. Eco-safe synthesis of AgNPs by 25% and 50% semipurified enzyme was demonstrated, leading to the formation of well-dispersed cubic to rounded particles with 6.51 ± 5.12 and 2.51 ± 3.45 nm size ranges, and UV analysis exhibited characteristic peaks at wavelengths of 416–404 nm, respectively. In addition, good peaks with particle size means of 96.20–82.30 nm and zeta potentials of –58.3 and –98.5 mv were observed by DLS analysis. The FTIR characterization showed the proteins' responsibility for the biosynthesized AgNPs, as shown from the obtained bands at 3,849.22, 3,440.39, 1,637.27, 1,432.85, 1,159.01, 1,031.73, 597.825, and 520.686 cm⁻¹. The antimicrobial results showed potential activity against Gram-positive *S. aureus*, Gram-negative *E. coli* (15–17 mm), and fungi *A. niger* and *F. solani* (11–13 mm). The antimicrobial properties demonstrated by the biosynthesized AgNPs can be applied as antimicrobial agents for some biomedical applications.

ACKNOWLEDGMENTS

The authors extend their appreciation to the Deanship of Scientific Research, University of Hafr Al Batin, for funding this work through Research Group Project No. 0006-1443-S.

CONFLICTS OF INTEREST

The authors declare that they have no conflicts of interest.

AUTHOR CONTRIBUTIONS

All authors made substantial contributions to conception and design, acquisition of data, or analysis and interpretation of data; took part in drafting the article or revising it critically for important intellectual content; agreed to submit to the current journal; gave final approval of the version to be published; and agree to be accountable for all aspects of the work. All the authors are eligible to be an author as per the international committee of medical journal editors (ICMJE) requirements/guidelines.

ETHICAL APPROVALS

This study does not involve experiments on animals or human subjects.

DATA AVAILABILITY

All data generated and analyzed are included within this research article.

PUBLISHER'S NOTE

This journal remains neutral with regard to jurisdictional claims in published institutional affiliation.

REFERENCES

- Abd El Aty AA, Ammar HA. Potential characterization and antimicrobial applications of newly bio-synthesized silver and copper nanoparticles using the novel marine-derived fungus *Alternaria tenuissima* KM651985. *Res J BioTechnol*, 2016; 11(8):71–82.
- Abd El Aty AA, El-Shamy AR, Atalla SMM, El-Diwany AI, Hamed ER. Screening of fungal isolates for laccase enzyme production from marine sources. *Res J Pharm Biol Chem Sci*, 2015; 6:221–8.
- Abd El Aty AA, Hamed ER, El-Beih AA, El-Diwany AI. Induction and enhancement of the novel marine-derived *Alternaria tenuissima* KM651985 laccase enzyme using response surface methodology: application to azo and triphenylmethane dyes decolorization. *J Appl Pharm Sci*, 2016; 6(4):6–14.
- Abd El Aty AA, Mohamed AA, Zohair MM, Soliman AAF. Statistically controlled biogenesis of silver nano-size by *Penicillium chrysogenum* MF318506 for biomedical application. *Biocatal Agric Biotechnol*, 2020; 25:101592; doi:10.1016/j.bcab.2020.101592
- Abd El Aty AA, Mostafa FA. Effect of various media and supplements on laccase activity and its application in dyes decolorization. *Malays J Microbiol*, 2013; 9(2):166–75.

- Abd El Aty AA, Mostafa FA, Hassan ME, Hamed ER, Esawy MA. Covalent immobilization of *Alternaria tenuissima* KM651985 laccase and some applied aspects. *Biocatal Agric Biotechnol*, 2017; 9:74–81.
- Abd El Aty AA, Shehata AN, Shaheen TI. Production and sequential optimization of *Bacillus subtilis* MF467279 pullulanase by statistical experimental designs and evaluation of its desizing efficiency. *Biocatal Agric Biotechnol*, 2018; 14:375–85.
- Abd El Aty AA, Zohair MM. Green-synthesis and optimization of an eco-friendly nanobiofungicide from *Bacillus amyloliquefaciens* MH046937 with antimicrobial potential against phytopathogens. *Environ Nanotechnol Monit Manage*, 2020; 14:100309; doi:10.1016/j.enmm.2020.100309
- Adelere IA, Lateef A. A novel approach to the green synthesis of metallic nanoparticles: the use of agro-wastes, enzymes, and pigments. *Nanotechnol Rev*, 2016; 5(6):567–87.
- Alshammari SO, Abd El Aty AA. Statically controlled mycogenic-synthesis of novel biologically active silver-nanoparticles using Hafr Al-Batin desert truffles and its antimicrobial efficacy against pathogens. *Saudi J Biol Sci*, 2022; 29:103334; doi:10.1016/j.sjbs.2022.103334
- Ammar HA, Abd El Aty AA, El Awdan SA. Extracellular myco-synthesis of nano-silver using the fermentable yeasts *Pichia kudriavzevii* HA-NY2 and *Saccharomyces uvarum* HA-NY3, and their effective biomedical applications. *Bioprocess Biosyst Eng*, 2021; 44:841–54; doi:10.1007/s00449-020-02494-3
- Bassanini I, Ferrandi EE, Riva S, Monti D. Biocatalysis with laccases: an updated overview. *Catalysts*, 2021; 11(26):1–30; doi:10.3390/catal11010026
- Behera A, Pradhan SP, Ahmed FK, Abd-Elsalam KA. Chapter 28-enzymatic synthesis of silver nanoparticles: mechanisms, and applications. Green synthesis of silver nanomaterials nanobiotechnology for plant protection, pp 699–756, 2022; doi:10.1016/B978-0-12-824508-8.00030-7
- Bhat R, Deshpande R, Ganachari SV, Huh DS, Venkataraman A. Photo-irradiated biosynthesis of silver nanoparticles using edible mushroom *Pleurotus florida* and their antibacterial activity. *Bioinorg Chem Appl*, 2011; 2011:650979.
- Chaurasia PK, Bharati SL, Yadava S. Nano-reduction of gold and silver ions: a perspective on the fate of microbial laccases as potential biocatalysts in the synthesis of metals (gold and silver) nano-particles. *Curr Res Microbial Sci*, 2022; 3:100098; doi:10.1016/j.crmicr.2021.100098
- Chawachart N, Khanongnuch C, Watanabe T, Lumyong S. Rice bran as an efficient substrate for laccase production from thermotolerant basidiomycete *Coriolus versicolor* strain RC3. *Fungal Divers*, 2004; 15:23–32.
- Cottenie A, Verloo L, Kiens L, Velghe G, Camerlynch R. Chemical analysis of plants and soils. Laboratory of Analytical and Agrochemistry, Ghent, Belgium, 1982.
- Devasia S, Nair AJ. Screening of potent laccase producing organisms based on the oxidation pattern of different phenolic substrates. *Int J Curr Microbiol App Sci*, 2016; 5(5):127–37.
- Eid AM, Fouda A, Niedbala G, Hassan SE-D, Salem SS, Abdo AM, Hetta HF, Shaheen TI. Endophytic *Streptomyces laurentii* mediated green synthesis of Ag-NPs with antibacterial and anticancer properties for developing functional textile fabric properties. *Antibiotics*, 2020; 9:641.
- Elegbede JA, Lateef A, Azeed MA, Asafa TB, Yekeen TA, Oladipo IC, Adebayo EA, Beukes LS, Gueguim-Kana EB. Fungal xylanases-mediated synthesis of silver nanoparticles for catalytic and biomedical applications. *IET Nanobiotechnol*, 2018; 12(6):857–63.
- Eltarahony M, Zaki S, El-Haleem DA. Concurrent synthesis of zero-and one-dimensional, spherical, rod-, needle-, and wire-shaped CuO nanoparticles by *Proteus mirabilis* 10B. *J Nanomater*, 2018; 2018:1849616; doi:10.1155/2018/1849616
- Eltarahony M, Zaki S, Abd-El-Haleem D. Aerobic and anaerobic removal of lead and mercury via calcium carbonate precipitation mediated by statistically optimized nitrate reductases. *Sci Rep*, 2020; 10:4029; doi:10.1038/s41598-020-60951-1
- Eltarahony M, Ibrahim A, El-shall H, Ibrahim E, Althobaiti F, Fayad E. Antibacterial, antifungal and antibiofilm activities of silver nanoparticles supported by crude bioactive metabolites of bionanofactories isolated from lake mariout. *Molecules*, 2021; 26:3027; doi:10.3390/molecules26103027
- Elyamny S, Eltarahony M, Abu-Serie M, Nabil MM, Kashyout AEHB. One-pot fabrication of Ag @ Ag₂O core-shell nanostructures for biosafe antimicrobial and antibiofilm applications. *Sci Rep*, 2021; 11:22543.
- Faramarzi MA, Forootanfar H. Biosynthesis and characterization of gold nanoparticles produced by laccase from *Paraconiothyrium variabile*. *Colloids Surf B Biointerf*, 2011; 87:23–7.
- Gopinath V, Velusamy P. Extracellular biosynthesis of silver nanoparticles using *Bacillus* sp. GP-23 and evaluation of their antifungal activity towards *Fusarium oxysporum*. *Spectrochim Acta A Mol Biomol Spectrosc*, 2013; 106:170–4.
- Ibrahim A, El-Fakharany EM, Abu-Serie MM, ElKady MF, Eltarahony M. Methyl orange biodegradation by immobilized consortium microspheres: experimental design approach, toxicity study and bioaugmentation potential. *Biology*, 2022; 11:76; doi:10.3390/biology11010076
- Kumar SA, Abyaneh MK, Gosavi SW, Kulkarni SK, Ahmad A, Khan MI. Sulfite reductase-mediated synthesis of gold nanoparticles capped with phytochelatin. *Biotechnol Appl Biochem*, 2007; 47:191–5.
- Lateef A, Adeeyo AO. Green synthesis and antibacterial activities of silver nanoparticles using extracellular laccase of *Lentinus edodes*. *Not Sci Biol*, 2015; 7:405–11; doi:10.15835/nsb.7.4.9643
- Lateef A, Akande MA, Ojo SA, Folarin BI, Gueguim-kana EB, Beukes LS. Paper wasp nest-mediated biosynthesis of silver nanoparticles for antimicrobial, catalytic, anticoagulant, and thrombolytic applications. *3 Biotech*, 2016; 6:140.
- Lowry OH, Rosebrough NJ, Farr AL, Randall RJ. Protein measurement with folin phenol reagent. *J Biol Chem*, 1951; 193:265–75.
- Mayolo-Deloisa K, Gonz´alez-Gonz´alez M, Rito-Palomares M. Laccases in food industry: bioprocessing, potential industrial and biotechnological applications. *Front Bioeng Biotechnol*, 2020; 8:222; doi:10.3389/fbioe.2020.00222
- Mostafa FA, Abd El Aty AA. Thermodynamics enhancement of *Alternaria tenuissima* KM651985 laccase by covalent coupling to polysaccharides and its applications. *Int J Biol Macromol*, 2018; 120:222–9.
- Mulvaney P. Surface plasmon spectroscopy of nanosized metal particles. *Langmuir*, 1996; 12:788–800.
- Munoz C, Guillen F, Martinez AT, Martinez MJ. Induction and characterization of laccase in the linnolytic fungus *Pleurotus eryngii*. *Curr Microbiol*, 1997; 34:1–5.
- Muthukumarasamy NP, Jackson B, Raj AJ, Sevanan M. Production of extracellular laccase from *Bacillus subtilis* MTCC 2414 using agroresidues as a potential substrate. *Biochem Res Int*, 2015; 2015:765190; doi:10.1155/2015/765190
- Ovais M, Khalil AT, Ayaz M, Ahmad I, Nethi SK, Mukherjee S. Biosynthesis of metal nanoparticles via microbial enzymes: a mechanistic approach. *Int J Mol Sci*, 2018; 19:4100; doi:10.3390/ijms1912410.
- Patel H, Gupte A. Optimization of different culture conditions for enhanced laccase production and its purification from *Tricholoma giganteum* AGHP. *Bioresour Bioprocess*, 2016; 3:11; doi:10.1186/s40643-016-0088-6
- Rai T, Panda D. An extracellular enzyme synthesizes narrow sized silver nanoparticles in both water and methanol. *Chem Phys Lett*, 2015; 623:108–12.
- Raju D, Paneliya N, Mehta UJ. Extracellular synthesis of silver nanoparticles using living peanut seedling. *Appl Nanosci*, 2014; 4:875–9; doi:10.1007/s13204-013-0269-y
- Rangnekar A, Sarma TK, Singh AK, Deka J, Ramesh A, Chattopadhyay A. Retention of enzymatic activity of α -amylase in the reductive synthesis of gold nanoparticles. *Langmuir*, 2007; 23:5700–6.
- Sanket S, Das SK. Role of enzymes in synthesis of nanoparticles. In: Thatoi H, Mohapatra S, Das SK (eds.). *Bioprospecting of enzymes in industry, healthcare and sustainable environment*, Springer, The Gateway, Singapore, pp 139–53, 2021; doi:10.1007/978-981-33-4195-1_7
- Sanghi R, Verma P, Puri S. Enzymatic formation of gold nanoparticles using *Phanerochaete chrysosporium*. *Adv Chem Eng Sci*, 2011; 1:154–62.

Shaheen TI, Abd El Aty AA. *In-situ* green myco-synthesis of silver nanoparticles onto cotton fabrics for broad spectrum antimicrobial activity. *Int J Biol Macromol*, 2018; 118:2121–30.

Shaligram NS, Singh SK, Singhal RS, Szakacs G, Pandey A. Effect of precultural and nutritional parameters on compactin production by solid state fermentation. *J Microbiol Biotechnol*, 2009; 19:690–7.

Shehata AN, Abd El Aty AA. Optimization of process parameters by statistical experimental designs for the production of naringinase enzyme by marine fungi. *Int J Chem Eng*, 2014; 2014:273523; doi:10.1155/2014/273523

Sousa AC, Martins LO, Robalo MP. Laccases: versatile biocatalysts for the synthesis of heterocyclic cores. *Molecules*, 2021; 26(12):3719; doi:10.3390/molecules26123719

Thirumurugan A, Tomy NA, Kumar HP, Prakash P. Biological synthesis of silver nanoparticles by *Lantana camara* leaf extracts. *Int J Nanomater Bioresour*, 2011; 1:22–4.

Tortella GR, Rubilar O, Gianfreda L, Valenzuela E, Diez MC. Enzymatic characterization of Chilean native wood-rotting fungi for potential use in the bioremediation of polluted environments with chlorophenols. *World J Microbiol Biotechnol*, 2008; 12:2805–18.

How to cite this article:

Alharbi R M, Alshammari SO, Abd El Aty AA. Statically improved fungal laccase-mediated biogenesis of silver nanoparticles with antimicrobial applications. *J Appl Pharm Sci*, 2023; 13(01):241–253.